Marbun, B. T. H.; Ridwan, R. H.; Nugraha, H. S.; Sinaga, S. Z.; Purbantanu, B. A.

Article

Casing setting depth and design of production well in water-dominated geothermal system with 330 °C reservoir temperature

Energy Reports

Provided in Cooperation with:
Elsevier

Suggested Citation: Marbun, B. T. H.; Ridwan, R. H.; Nugraha, H. S.; Sinaga, S. Z.; Purbantanu, B. A. (2020) : Casing setting depth and design of production well in water-dominated geothermal system with 330 °C reservoir temperature, Energy Reports, ISSN 2352-4847, Elsevier, Amsterdam, Vol. 6, pp. 582-593,
https://doi.org/10.1016/j.egyr.2020.02.013

This Version is available at:
https://hdl.handle.net/10419/244060

Energy Reports 6 (2020) 582–593

Contents lists available at ScienceDirect

Energy Reports

journal homepage: www.elsevier.com/locate/egyr

Research paper

Casing setting depth and design of production well in water-dominated geothermal system with 330 °C reservoir temperature

B.T.H. Marbun [a,*], R.H. Ridwan [b], H.S. Nugraha [c], S.Z. Sinaga [a], B.A. Purbantanu [a]

[a] Petroleum Engineering Study Program, Bandung Institute of Technology, Indonesia
[b] PT Geo Dipa Energi, Jakarta, Indonesia
[c] Directorate General of New and Renewable Energy and Energy Conservation of the Ministry of Energy and Mineral Resources, Indonesia

ARTICLE INFO

Article history:
Received 26 August 2019
Received in revised form 13 January 2020
Accepted 19 February 2020
Available online xxxx

Keywords:
Casing design
Casing setting depth
Geothermal production well
Water-dominated geothermal reservoir

ABSTRACT

Casing, with its two main elements: casing setting depth and casing design, is one of well barrier elements playing a significant role for geothermal well integrity. All of the internal and external loads experienced by the casing from its installation into the well until the end phase of well, called plug and abandonment, have to be calculated precisely. Moreover, the casing must be able to withstand the geothermal environment: high-temperature, high-strength rock, highly-fractured formation, corrosive fluid, and under-saturated pressure. Therefore, the casing specification can be properly determined based on the technical and economic considerations to achieve a high quality of well integrity and endurance starting from drilling and completion, production, maintenance (well intervention, and workover), conversion into an injection well or vice-versa, and plug and abandon (P&A).

This research study discussed the production well HCE29 in Dieng Field, Indonesia, characterized by a water-dominated geothermal system with temperature of up to 330 °C and pressure of up to 19.4 MPa. After the well was drilled and completed, the casing failure was identified. This study consisted of analysis and re-calculation of this well at the phases of drilling, completion, production, and maintenance to improve the casing setting depth and design method. The results show that the casing failure occurred in this well. In addition, this study improved the Philippines' method used for re-calculation of casing setting depth and the casing design evaluation method.

1. Introduction

Well integrity is a crucial aspect that must be maintained through the lifecycle of a well, and one component of which, the casing, must be able to withstand all the internal and external loads. These loads include the invariable factors in the geothermal environment, such as high-temperature, high-strength rock, highly-fractured formation, corrosive fluid, and under-saturated pressure (Standards New Zealand, 2015; Hole, 2008). Thus, in the casing construction process of setting depth and design of a geothermal production well, these factors needed to be taken into account based on the environment where the well is located to ensure that casing failure does not happen (Standards New Zealand, 2015; Kaldal et al., 2015).

This study focused on casing construction in geothermal production well HCE29, in a water-dominated geothermal system Dieng Field, with temperature of up to 330 °C, pressure of up to 19.4 MPa, and corrosive substances (CO_2, H_2S, HCl, and NH_4Cl) contained in geothermal fluids with pH of 4–5 (PT Geo Dipa Energi, 2019; Marbun, 2013). The existing casing installed in this well was designed based only on the drilling load assumption, and the casing setting depth and design were performed independently of each other. Later on, during production, casing failure was discovered.

However, an existing method of casing setting depth, the Philippines' method (Sarmiento, 2007), was not deemed suitable enough to be applied in well HCE29 because this method only considers one parameter – the reservoir temperature 220 °C – without taking into account other factors such as geological conditions, lithology, risks and hazards, corrosion potential, production, and various loads in each operation during the life cycle of the well.

Therefore, the objective of this study was twofold. Firstly, to develop a better casing setting depth and design which were dependent on each other and were performed iteratively based on the lesson learned from the well HCE29 history so that the design method for these can be improved. Secondly, to improve

* Correspondence to: Jalan Ganesha 10, Bandung 40132, Indonesia.
E-mail address: bonar.marbun@tm.itb.ac.id (B.T.H. Marbun).

https://doi.org/10.1016/j.egyr.2020.02.013

the Philippines' method by adding variables other than the reservoir temperature to better accommodate existing conditions in well HCE29, including drilling (trajectory, dogleg severity, well schematic, and casing), lithology, geological condition, pressure and temperature, production, and well problems and hazards. Thus, the analysis done to this well was conducted in three stages: review the former casing construction in this well, re-calculate the casing setting depth and design, and evaluate the methodology using this improved Philippines' method.

It is also worth noting that this study was the continuation of a previous research study regarding the identification of casing failure in this field (Marbun et al., 2019). The previous study assessed the integrity of the two geothermal abandoned wells, re-calculated the wells' design with consideration of the effect of inclination and azimuth, and proposed the well intervention and workover plan, and together with the findings of this study, the result can be used for evaluating the casing failure in well HCE29.

2. Literature review

2.1. Casing setting depth

There are different methods of casing setting depth based on the characteristics of the geothermal well. These include New Zealand's, Iceland's, and Philippines' methods, and all are used in high-temperature geothermal wells.

New Zealand's method is applied with the assumption that the well is filled with steam, and the minimum setting depth of the casing is determined based on the boiling point depth (BPD) curve and overburden pressure (Standards New Zealand, 1991; Hossein-Pourazad, 2005). Another method – Iceland's method – is used in a flowing well by assuming an inflow from the bottom of the well (Standards New Zealand, 1991; Hossein-Pourazad, 2005). Two-phase flow occurs at the bottom of the well. The minimum setting depth of the casing is determined based on the BPD curve and the pressure from the heavy drilling fluid. Secondly, Iceland's method considers the actual or most-likely case for downhole pressure and temperature of the well (Standards New Zealand, 1991; Hossein-Pourazad, 2005). Two-phase flow occurs on the way the fluid flow in the hole. The minimum setting depth of the casing is determined based on the BPD curve and the pressure from pure water.

Another common method of casing setting depth – the Philippines' method – is used in geothermal reservoirs with dominant water characteristic. The production casing shoe is set at the top of the reservoir to isolate it from cold aquifers because they can cause difficulties in initiating the flow of geothermal fluid through the well due to a substantial pressure drop (Sarmiento, 2007). To prevent this, the production casing shoe is set at the depth with a minimum temperature of 220 °C. To design the casing setting depth, the pore and overburden pressure are plotted in the graph as the lower and upper boundaries. Subsequently, the depth with a temperature of 220 °C is determined based on temperature survey from offset wells or temperature simulation from exploratory wells. The Philippines' method considers only the reservoir temperature of 220 °C for casing setting depth as can be seen in Fig. 1.

It can be seen from Fig. 1 that the surface casing and production liner are set by extrapolating the line up and down the production casing depth. The criteria of well can be analyzed using the Philippine's' method and thus, this method was deemed suitable to be applied in Dieng Field.

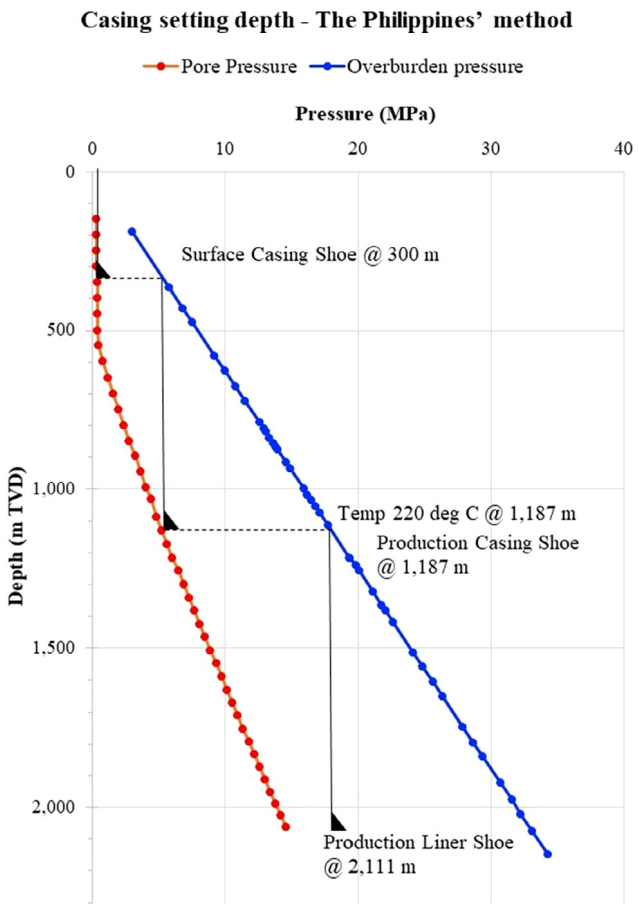

Fig. 1. An example of casing setting depth using the Philippines' method (Marbun, 2013).

2.2. Casing design load case identification

Generally, casing design load case identification of hydrocarbon wells and geothermal wells are different. In a hydrocarbon well, burst, collapse, and axial tension load with various scenarios, for instance maximum load or minimum load needs to be considered (Bourgoyne Jr. et al., 1986; American Petroleum Institute (API), 2011; Kaldal et al., 2015). These loads are calculated based on the pore pressure, the fluid pressure inside the casing, the weight of the casing, and the tensile load (Hole, 2008). The grades and types of the casing in hydrocarbon well are then selected based on loads design and pre-determined design factor or safety factor (Bourgoyne Jr. et al., 1986; American Petroleum Institute (API), 2011). The design factor usually depends on various aspects such as well and formation difficulty and companies' standard operating procedure (SOP).

On the other hand, in geothermal wells, it is mandatory to consider the high-temperature gradient, since it causes thermal stress and material strength degradation (Nicholson, 1984; Southon, 2005; Karlsson, 1978). This consideration should be done not only while in the drilling stage, but even more crucial in the production stage, when the thermal stress increases significantly. The high-temperature effect is considered in yield strength correction factor that reduces the casing strength (Dench, 1970; Nicholson, 1984).

Additionally, in a geothermal well, the internal and external loads considered in casing design load case identification are different from that of a hydrocarbon well. In the latter, the hydrocarbon is produced through the production tubing, while in the

former, the fluid is produced through the production casing and production liner. This includes well intervention and workover in the geothermal well that is carried out through production casing and production liner. Moreover, in a geothermal environment, other specific conditions such as under pressure strata, lost circulation zones, and high dogleg severity (DLS) zones, must also be considered. These conditions significantly affect the axial and lateral loads and forces experienced by the casing during the drilling and the production of the geothermal well, and the maximum load concept is used in burst, collapse, and tension load design (Rahman and Chilingarian, 1995; Bourgoyne Jr. et al., 1986; Byrom, 2007). Therefore, all loads in each section during the life cycle of the well must be defined and the maximum load scenario is taken into consideration when determining the internal and external load.

Similar method of applying design factor as that of hydrocarbon wells is also applied in geothermal wells, sometimes with higher design factor than in the hydrocarbon well casing design due to the high thermal stress consideration (Hole, 2008; Kaldal et al., 2015).

2.2.1. High-temperature effect

The high-temperature effect in geothermal wells must be considered in designing the geothermal casing since it reduces the yield strength of the casing (Dench, 1970; Nicholson, 1984). The yield correction factor is based on New Zealand Standard NZS 2403:2015 (Standards New Zealand, 2015), which is then applied to the burst, collapse, and tension rating of the casing.

2.2.2. Burst load design

The maximum burst load occurs when the cement slurry is pumped into the well. The internal pressure is calculated with the following equation considering the hydrostatic pressure of the cement slurry:

$$P_i = P_{sur} + G_{ce} \times D \tag{1}$$

where:
P_i = internal pressure (MPa)
P_{sur} = surface pumping pressure (MPa)
G_{ce} = cement slurry pressure gradient (MPa/m)
D = depth of casing shoe (m)
The pore pressure data is used for the external pressure calculation. The following equation is used for the external pressure calculation:

$$P_e = G_{fp} \times D \tag{2}$$

where:
P_e = external pressure (MPa)
G_{fp} = pore pressure gradient (MPa/m)
D = depth of casing shoe (m)
The burst load design is then determined based on the resultant between the internal pressure deducted by the external pressure and multiplied by the design factor.

2.2.3. Collapse load design

The maximum collapse load occurs when the cement slurry fills the annulus during the cementing operation. This situation is aggravated when a total lost circulation occurs causing the inside well to be empty. The hydrostatic pressure of the cement slurry is assumed as the external pressure. Therefore, the external pressure is expressed as follows:

$$P_e = G_{ce} \times D \tag{3}$$

where:
P_e = external pressure (MPa)
G_{ce} = cement slurry pressure gradient (MPa/m)
D = depth of casing shoe (m)
The lost circulation rate in geothermal wells is more massive than that in hydrocarbon wells. Due to lost circulation, there is no fluid inside the casing, causing the internal pressure to be zero. Lost circulation affects the drilling fluid and cement circulation criteria in the collapse load calculation since the external pressure is increasing. The collapse load design is determined based on the resultant between the external pressure deducted by the internal pressure and multiplied by the design factor.

2.2.4. Axial load design

Tension load is generated from the weight of the casing and the force applied axially. Based on the maximum load concept, the maximum tension load occurs due to its own weight minus the buoyancy after the casing running and before the cementing operation.

$$BF = 1 - \frac{MW}{7848.6} \tag{4}$$

where:
BF = buoyancy factor (dimensionless)
MW = mud weight (kg/m^3)
In lost circulation zones, it is necessary to control the drilling fluid and cement pumping rate to keep the optimum fluid column. The buoyancy force fluctuates according to the fluid column height in the well and will affect the axial load experienced by the casing. Furthermore, this affects the cutting transportation to the surface to avoid the cutting accumulation in the well that can cause stuck pipe. Torque and drag during running casing will also be affected by the fluid column height and lost circulation zones. The tension design load is calculated based on the weight of the casing and multiplied by the design factor.

2.2.5. Thermal expansion of the trapped fluid

The pressure increase of trapped fluid in the annulus production-surface casing can cause the production casing to collapse (Hole, 2008). The formation fluid fills the empty column of the annulus and during the production phase, the thermal expansion of the fluid causes the pressure to increase. This phenomenon is similar to that of the annular pressure build-up (APB) in a hydrocarbon well, particularly in deepwater well (Zhang et al., 2019; Dong and Chen, 2017). According to Hole (2008), the thermal expansion of water can cause a pressure increase of approximately 1.6 MPa/°C.

Thus, the casing is ideally fully cemented to prevent the presence of trapped fluid in the annulus. Moreover, to maintain the production casing integrity, it is compulsory for the selected production casing to have a higher collapse rating than the burst rating of the outer casing (e.g. surface casing and intermediate casing) (Hole, 2008). Hole (2008) suggests that the ratio of the collapse rating of the production casing to the burst rating of the outer string to be no less than 1.2.

2.3. Material selection

In hydrocarbon wells, material selection is considered as an effective method to prevent corrosion (Kermani et al., 2005; Smith and DeWaard, 2005). The material is selected based on the type of corrosive substances present in the well (e.g., CO_2 or H_2S), predicted corrosion mechanism, and various factors such as pressure, pH, and temperature. Various types of casing material is now available in the industry to help prevent corrosion from happening in hydrocarbon wells such as carbon steel, stainless steel, and other corrosion resistant alloy (CRA) containing varying amounts of iron, nickel, chromium, and molybdenum (Nogara and Zarrouk, 2018b). Similar to hydrocarbon wells, geothermal

Table 1
Range of Cr equivalent value for several API casing grade (Ekasari and Marbun, 2015; American Petroleum Institute (API), 2011).

Range of Cr_{eq} value			
Grade casing (API 5CT)		Min	Max
Group 1	H40	−8.5	−7.5
	J55	−6	−5.4
	K55	−6	−5
	N80–1	−2	−1.5
	N80Q	−2	−1.5
Group 2	M65	−5.5	−4.3
	L80–1	−2.4	−1.8
	L80-9Cr	10	11.5
	L80-13Cr	11	12

production fluid often contains corrosive substances, albeit with a higher level of corrosiveness than that in hydrocarbon wells. These corrosive substances include acid sulfate (H_2S and HSO_4^-), chloride (HCl and NH_4Cl), ammonia (NH_3), carbonate (CO_3^{2-}), bicarbonate (HCO_3^-), carbon dioxide (CO_2), and oxygen (O_2) (Mahon et al., 2000; Nogara and Zarrouk, 2018a; Ellis and Conover, 1981). The presence of these corrosive substances in geothermal fluid, high temperature, pressure changes, and salinity leads to corrosion and casing damage (Nogara and Zarrouk, 2018a; Karlsdottir et al., 2015). Additionally, the combination of high temperature and pressure tends to accelerate the corrosion reaction, causing casing thickness reduction and eventually material strength degradation (Karlsdottir et al., 2015). The similar principle of material selection in hydrocarbon well is also applied in geothermal well casing design with the consideration of high-temperature, type of fluids and substances, and pH (Ekasari and Marbun, 2015; Cabrini et al., 2017; Kurata et al., 1995). Meticulous selection for casing materials is crucial as casing material selection is considered an effective method in preventing corrosion and prolonging the lifetime of the well.

One study related to casing material selection was done by Kurata et al. (1995) who performed an experimental corrosion test according to various geothermal deep wells conditions in Japan. They then developed a method to estimate the corrosion rate and to select the appropriate materials for geothermal production casing. Ekasari and Marbun (2015) later improved the method according to the geothermal well condition in Indonesia with the following equation:

$$\log(CR) = 2.981 - 2.912\left(Cr_{eq}\right) - 4.532\,(pH) - 25.052\left(\frac{1}{T}\right) \quad (5)$$

where:
CR = corrosion rate (mm/year)
Cr_{eq} = chromium equivalent
T = temperature (°C)
Based on Eq. (5), a diagram of Cr_{eq} versus temperature is plotted at a given corrosion rate and pH value. Using this diagram, the value of Cr_{eq} at a given temperature is determined. Kurata et al. (1995) derived an equation to correspond Cr_{eq} with the chemical composition of the casing:

$$Cr_{eq} = Cr - 13.73\,C + 1.598\,Si - 0.433\,Mn + 27.28\,P - 51.12\,S + 0.237\,Ni + 0.712\,Mo - 1.06\,Cu \quad (6)$$

where Cr: Chromium, C: Carbon, Si: Silicon, Mn: Manganese, P: Phosphorus, S: Sulfur, Ni: Nickel, Mo: Molybdenum, and Cu: Copper. By using Eq. (6), the range of Cr_{eq} value of the API casing grade material from API Spec 5CT was calculated (Kurata et al., 1995; American Petroleum Institute (API), 2011; Ekasari and Marbun, 2015).

Table 1 shows the Cr_{eq} value for several API casing grade.

Suitable materials for casing as seen from Table 1 was then selected by matching the result of Cr_{eq} value calculated with Eq. (5) with the range of Cr_{eq} value of the listed API casing grade in Table 1.

3. Methodology & overview of the well

3.1. Methodology

Well HCE29 was drilled and completed in 1997 (PT Geo Dipa Energi, 2019; Marbun, 2013). However, available data for this well is extremely limited. By collecting and identifying the limited available data, this study evaluated and analyzed the occurred casing failure problems in this well. With an iterative process, an improvement for casing setting depth and design was established. Fig. 2 shows the methodology of this study.

It can be seen from Fig. 2 that there are several stages in an iterative process used in the study, with the explanation as follows.

1. Identification of production well HCE29 based on limited available data: drilling (trajectory, dogleg severity, well schematic, and casing), lithology, geological condition, pressure and temperature, production, well problems and hazards.
2. Evaluation and analysis of the actual casing setting depth and design based on geothermal industrial practices and standards. These included New Zealand Standard (NZS) (Standards New Zealand, 2015, 1991), American Petroleum Institute (API) Spec 5CT (American Petroleum Institute (API), 2011), API Recommended Practice (RP) 7G (American Petroleum Institute (API), 1998), API Spec 10A (American Petroleum Institute (API), 2005), and American Standard Testing and Material (ASTM) 193 (American Standard Testing and Material (ASTM), 2017). API Spec 5CT and API RP 7G are designed for oil and gas environment that consider lower temperature than in a geothermal environment. The high-temperature effect was included in the analysis of this study.
3. Re-determination of the casing setting depth based on the improved Philippines' method.
   The casing setting depth of each section should consider all temperature variations during the life cycle of the well. The actual or estimated maximum temperature is then selected as the basis for casing setting depth. Due to the limitation of available data in this study, the casing setting depth evaluation using the improved Philippines' method considered various temperature survey data taken from before, during, and after the flow test. Other variables were also considered in the evaluation: drilling (trajectory, dogleg severity, well schematic, and casing), lithology, geological condition, pressure and temperature, production, and well problems and hazards (e.g., lost circulation zones) (PT Geo Dipa Energi, 2019; Marbun, 2013).
4. Re-calculation of the internal and external loads for all scenarios, including drilling and completion, production, maintenance (well intervention, and workover), conversion into an injection well or vice-versa, and plug and abandon (P&A).
   The loads calculation of each section of the casing should consider the maximum load based on the pressure and temperature variation during the life cycle of the well. The cementing operation is considered as the maximum load scenario for the casing design load case identification. There were no measurement and calculation of pore, fracture, and overburden pressure in this field. The pressure measurement from the pressure and the temperature

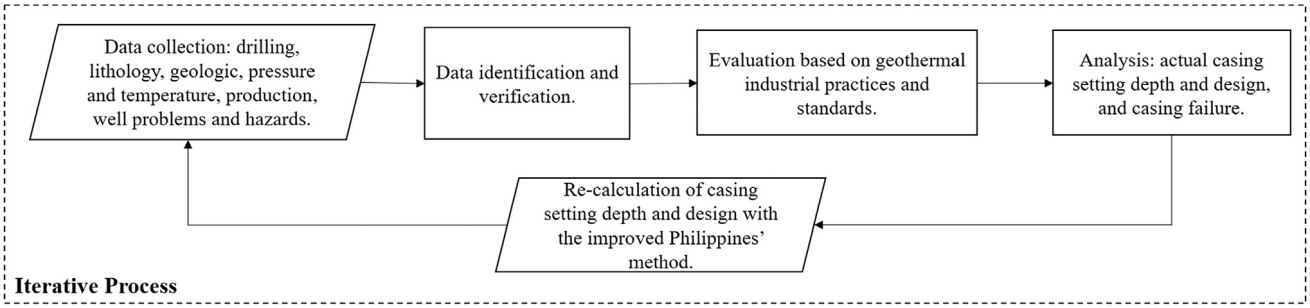

Fig. 2. The methodology of the study.

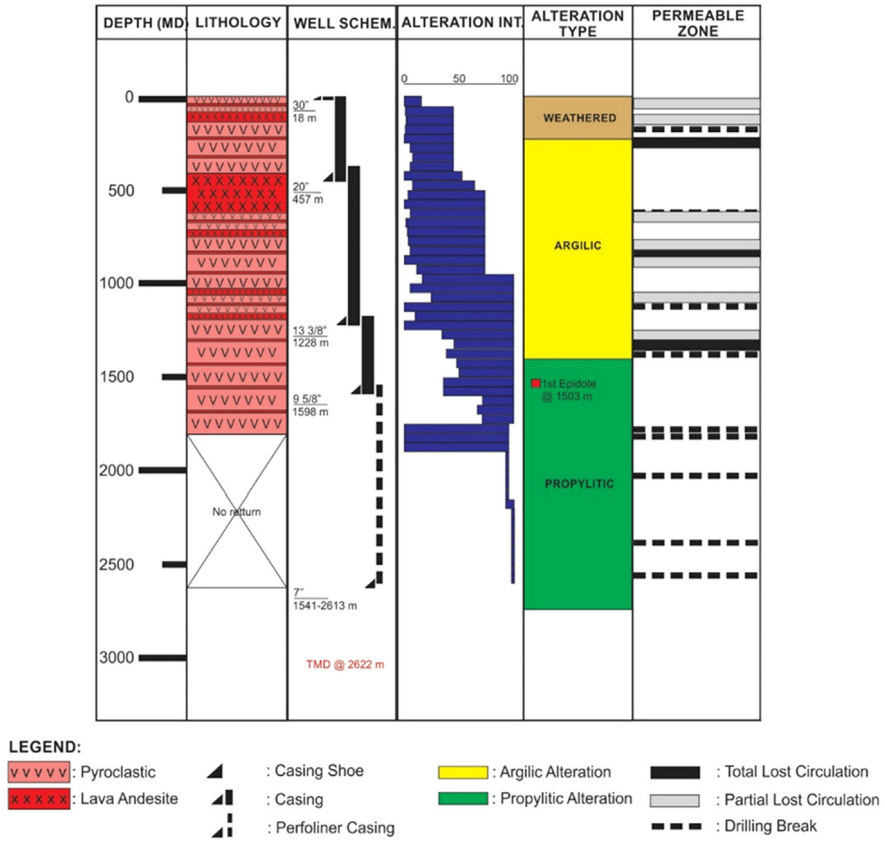

Fig. 3. Stratigraphy of the nearby well (PT Geo Dipa Energi, 2019).

survey data conducted after the drilling, before the flow test, during the flow test, and after the flow test operations was used as the basis for external pressure calculation. The range of the pressure gradient in this field, based on previous pressure and temperature survey data of well HCE29, was 0.0001–0.013 MPa/m (PT Geo Dipa Energi, 2019; Marbun, 2013). This data was used in calculating the internal and external loads. Based on the lesson learned, experiences in this field, and the geothermal industrial practices, the design factor used in this study were 1.2, 1.4, and 2.2, for burst, collapse, and tension load, respectively (Marbun, 2013; Hole, 2008). In this study, the yield correction factor was based on New Zealand Standard NZS 2403:2015 (Standards New Zealand, 2015). The thermal expansion of the trapped fluid and material selection were also performed in this study, which were not considered in the original design of this well.

5. Iterative process.

3.2. Overview of the well

Data gathered from the limited previous reports gave an overview of well HCE29, shown in Fig. 3 until Fig. 8 as follows. Fig. 3 shows the stratigraphy of the nearby well (PT Geo Dipa Energi, 2019).

Due to the limited available data, the available stratigraphy from the nearby well as seen in Fig. 3 was used as reference in this study. The stratigraphy was taken from a production well that is located approximately 2 km northeast of the well HCE29 in the same field area.

Fig. 4 shows the planned and actual trajectory and actual well schematic of well HCE29 (Standards New Zealand, 2015; Hole, 2008).

According to the last well investigation, the silica scaling issue was encountered in the production casing. Casing wear was also identified during the run of caliper log at the production casing: 860–870 m (up to 15%); 1057–1068 m (up to 30%); 1310–1430 m

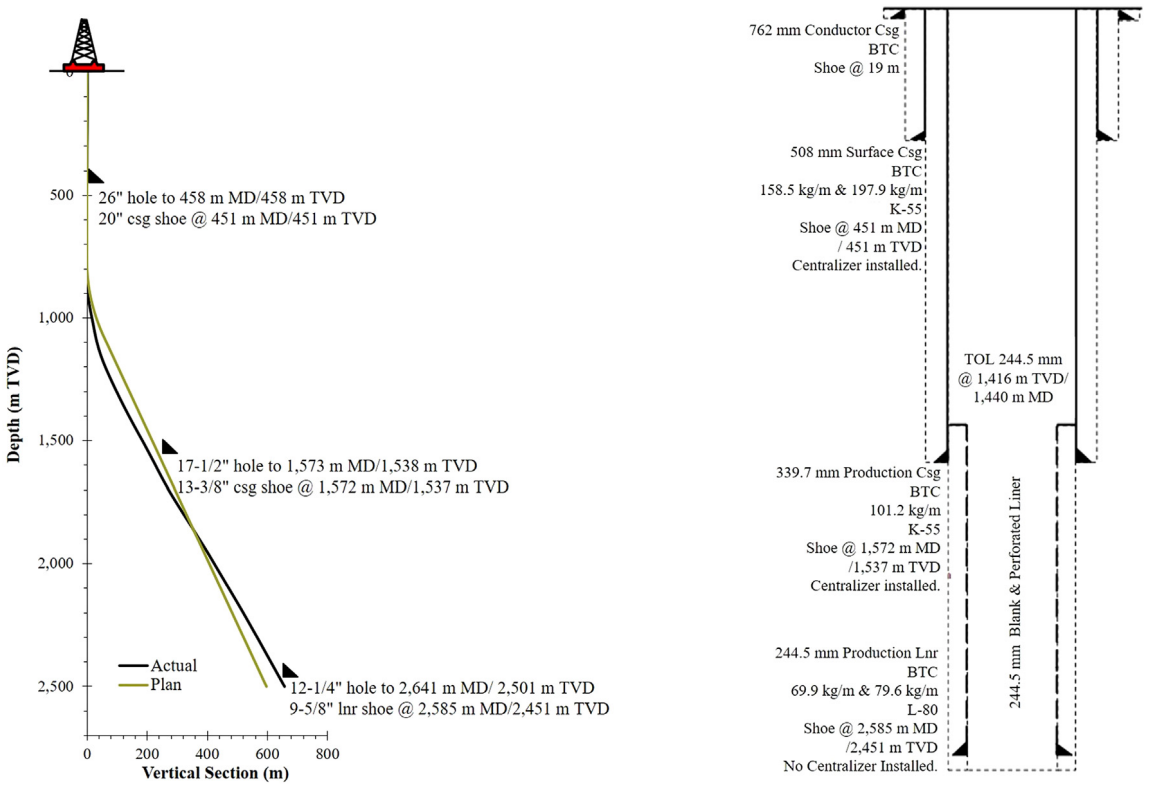

Fig. 4. Planned and actual trajectory (left) and actual schematic of the well (right) (PT Geo Dipa Energi, 2019; Marbun, 2013).

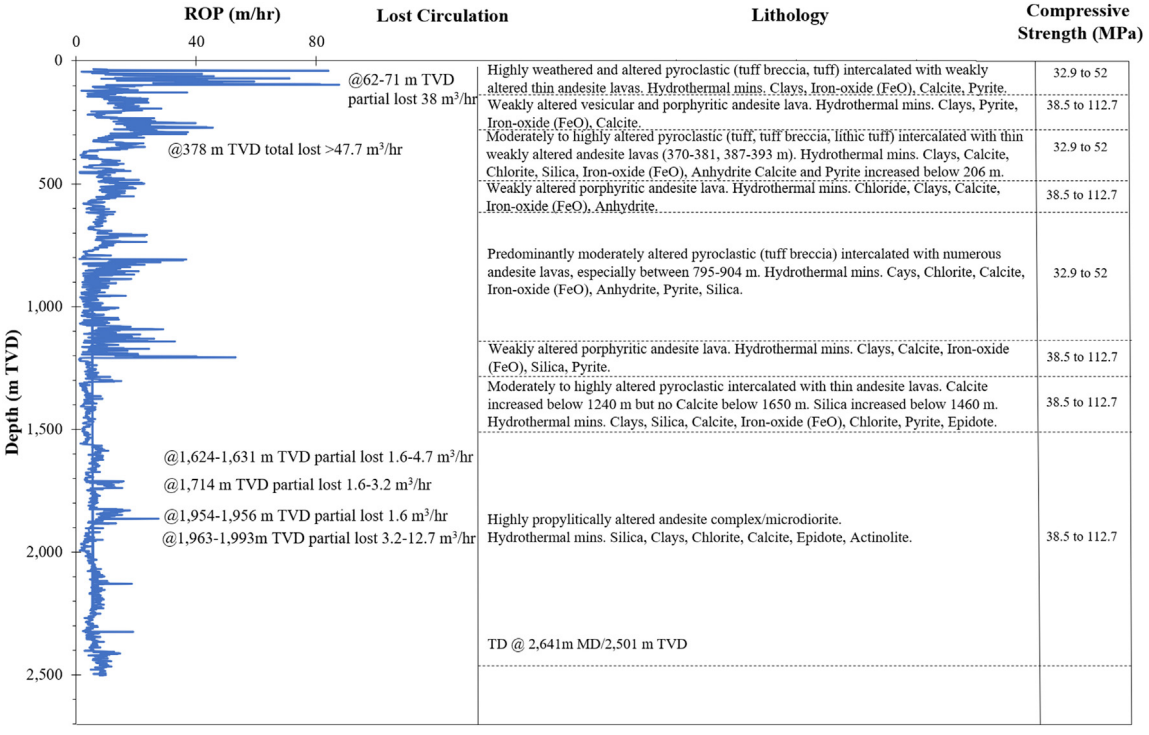

Fig. 5. ROP, lost circulation zones, lithology, and compressive strength of the lithology of the well (PT Geo Dipa Energi, 2019; Marbun, 2013; Perras and Diederichs, 2014; Dinçer et al., 2004).

(up to 25%). Casing leak was also reported, which allowed the shallow fluids to enter the well.

Fig. 5 shows the rate of penetration (ROP), lost circulation zones, lithology, and compressive strength of the lithology of the well.

In Fig. 5, the compressive strength data was not available and was obtained from the literature study (Perras and Diederichs, 2014; Dinçer et al., 2004). Fig. 6 shows four selected pressure and temperature survey data of well HCE29.

Table 2
Casing setting depth scenarios.

Comparison		Setting depth (m TVD)		
		Surface casing	Production casing	Production liner
Actual		451	1537	2451
Philippines' method	Based on pressure and temperature survey conducted 1 week before 1st flow test	600	1022	2451
	Based on pressure and temperature survey conducted during 1st flow test	175	1426	2451
	Based on pressure and temperature survey conducted 37 days after 1st flow test	275	906	2451

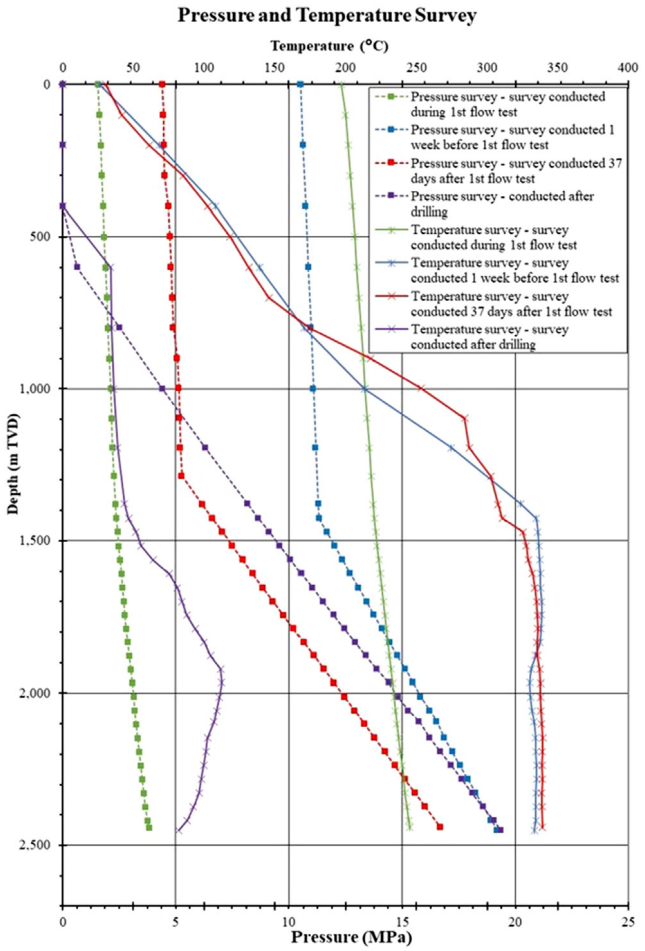

Fig. 6. Pressure and temperature data of the well (PT Geo Dipa Energi, 2019; Marbun, 2013).

The selection of four pressure and temperature survey data as seen in Fig. 6 was based on the extreme difference condition after drilling, before flow test, during flow test, and after flow test operations that affected the loads on the casing.

Fig. 7 shows the production data of the well for approximately the past two years.

In Fig. 7, the letters A, B, C, and D shows the different discharge time periods. The individual production data of well HC29 was not available because there was no continuous measurement (PT Geo Dipa Energi, 2019). The last updated well outputs were constructed based on tracer flow test (TFT) data as supplied in the well field assumption. According to this update, the monitoring data provided for the production period for this well was in actuality data computed for well HCE29 starting from the data measured on common separation facilities. The TFT result in 2012 was discussable because of the vast difference between the TFT 2012 with the other TFT results. The initial flow rate data was compared with the last flow rate data measured by TFTs to derive the average flow rate decline for wells without known (current) restrictions in the wellbore.

Fig. 8 shows the enthalpy vs. wellhead pressure (WHP) (left) and rate vs. WHP (right) graphs.

In Fig. 8, the TFT tests performed in 2012, 2015 and 2018 were included with the simulated OCs. The initial production potential of well HCE29 was 7.2 MW with 51 ton/h steam flow (PT Geo Dipa Energi, 2019). The well was initially a moderate producer with a flat curve and production enthalpy of 1630–1680 kJ/kg. Initial and production data also showed flat curves with a remarkable rate decline from the year 2004 to 2017–2018, showing clearly that these enthalpies were lower than those measured before field exploitation (PT Geo Dipa Energi, 2019). Based on the calculation done in 2006, the reservoir pressure of this well was 11 MPa, enthalpy 1450 kJ/kg, and permeability thickness (kh) 8.1 Darcy Meter. Pressure and temperature logs recorded under flowing conditions were available for this well, showing the two-phase conditions down to the bottom hole.

4. Analysis, result, and discussion

4.1. Analysis of DLS

Controlling the drilling fluid pumping rate was important when encountering the lost circulation zones. Due to severe lost circulation zones, the height of the drilling fluid column in the well was difficult to control. This caused the fluctuation of buoyancy force, torque, and drag of the drill string during the drilling operation, and it also led to a difficulty in controlling the direction and the inclination of the drilling, high DLS zones, bad borehole quality, and wellbore instability issues. Moreover, the cutting was not transported to the surface optimally and this led to cutting accumulation in the well that caused stuck pipe. Fig. 9 shows the analysis of DLS in this well. The high DLS zones are zones with DLS above 2 degree/30 m (Hole, 2008).

The high DLS and lost circulation zones as shown in Fig. 9 also affected the casing. The actual loads and forces that were experienced by the casing were higher than the casing design plan. This contributed to the casing failure that occurred after drilling operation and during the production of the well

4.2. Result of casing setting depth and design load case identification

The setting depth and design load case identification of the actual casing were re-calculated in this study using the Philippines' method. Table 2 shows the three scenarios of casing setting depth based on the pressure and temperature survey data from Fig. 6.

Based on analysis in Table 2, the optimization of casing setting depth according to the Philippines' method and experiences in this well is proposed. The setting depth of the surface casing was between 175–600 m TVD, the setting depth of the production

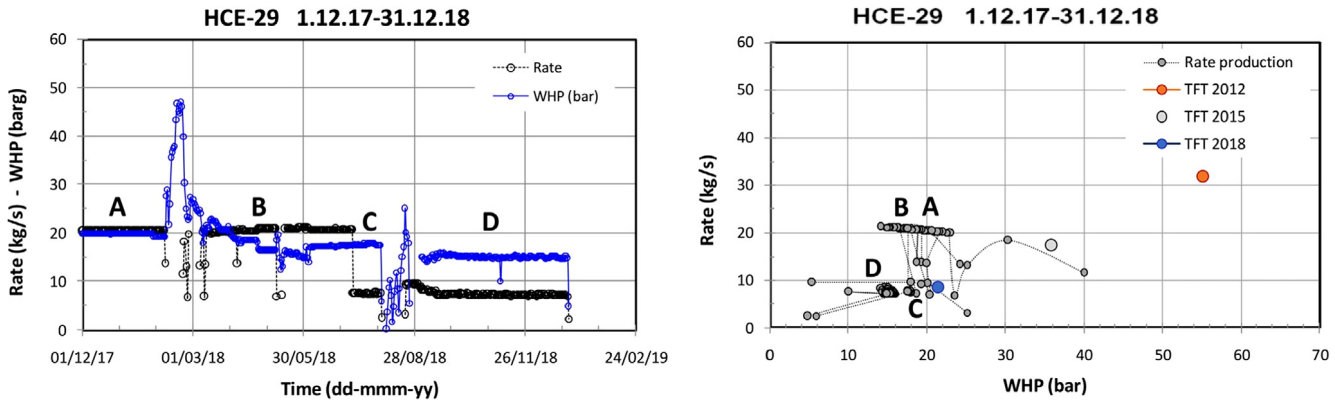

Fig. 7. Mass production rate and wellhead pressure (WHP) vs. time (left) Mass production rate vs. WHP of the well (right) (PT Geo Dipa Energi, 2019; Marbun, 2013).

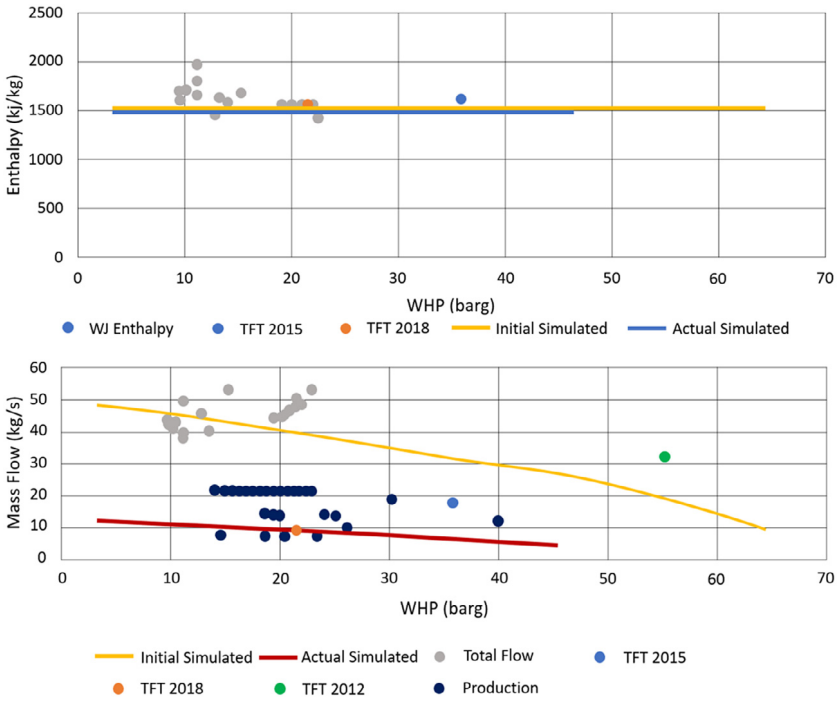

Fig. 8. Enthalpy vs. WHP (top) and rate vs. WHP (bottom) for initial and production data (PT Geo Dipa Energi, 2019; Marbun, 2013).

casing was between 906–1022 m TVD, and the setting depth of the production liner was at 2451 m TVD. An additional section of intermediate production casing/liner can be considered to be set between the setting depth of the production casing and the production liner. According to the analysis in Fig. 5, lost circulation zones were encountered at approximately 1600–2000 m TVD. The additional intermediate production casing/liner is considered to be set at approximately 2000 m TVD to seal the lost circulation zones and to optimize the drilling and production. To accommodate the additional intermediate production casing/liner and the requirement to install big casing at reservoir zones to optimize the production, the diameter casing selection is increased. Table 3 shows the analysis of the options for the proposed casing/liner diameter based on experience in this well.

In Table 3, the outer casing/liner diameter was then selected accordingly to accommodate the selected 244.5 mm innermost production liner.

The actual production casing installed in this well was K55 (101.2 kg/m) (PT Geo Dipa Energi, 2019; Marbun, 2013). The burst and collapse load of the production casing were re-calculated using Eqs. (1), (2), and (3). The design factor for burst and collapse load re-calculation were 1.2 and 1.4 respectively (Hole, 2008; Marbun, 2013). The maximum and minimum pressure gradient for internal and external pressure calculation in burst and collapse load case identification are shown in Table 4.

As can be seen in Table 4, the hydrostatic cement pressure gradient was 0.019 MPa/m. Based on the pressure and temperature survey data, the lowest pore pressure gradient was 0.0001 MPa/m for burst load case identification, while for collapse load case identification, there was no fluid inside the casing due to

Table 3
Diameter options for the proposed casing/liner.

Casing	Diameter (mm)
Conductor	1066.8; 914.4; 762
Surface casing	762; 609.6; 508; 473.1
Production casing	508; 473.1; 406.4
Additional intermediate production casing/liner	301.6; 298.5
Production liner	244.5

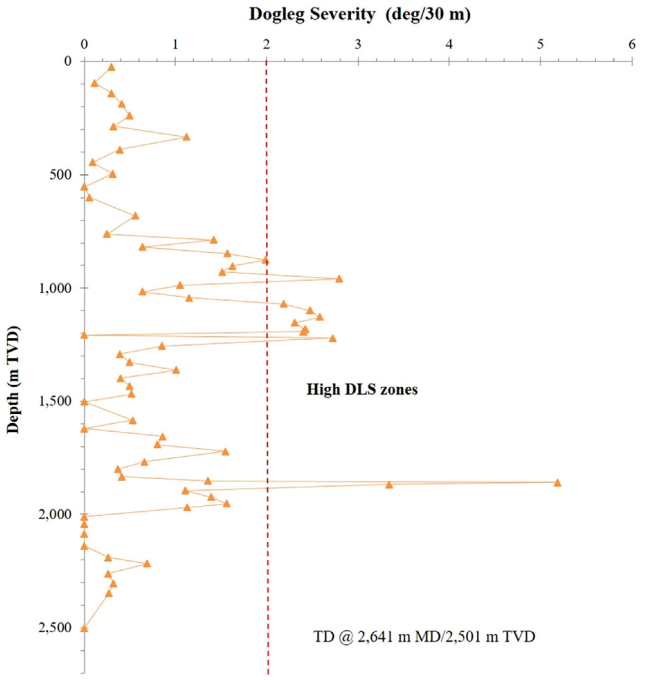

Fig. 9. DLS analysis of the well (PT Geo Dipa Energi, 2019; Marbun, 2013).

Table 4
Maximum and minimum pressure gradient for internal and external pressure calculation in burst and collapse load case identification (PT Geo Dipa Energi, 2019; Marbun, 2013).

Criteria calculation	Burst load	Collapse load
Pressure gradient for internal pressure calculation (MPa/m)	0.019	0
Pressure gradient for external pressure calculation (MPa/m)	0.0001	0.019

Table 5
The buoyancy factor fluctuation due to lost circulation.

Rate of lost circulation (%)	Buoyancy factor
0	0.85
50%	0.93
100%	1

Table 6
Summary of actual casing design load case identification of the well.

Casing	Failure in actual casing
Surface casing	Failure
Production casing	Failure
Production liner	Failure

total lost circulation (internal pressure 0). The yield correction factor for the high-temperature effect consideration was based on New Zealand Standard NZS 2403:2015 (Standards New Zealand, 2015). The yield correction factor was then applied to the burst and collapse rating of the casing.

Fig. 10 shows the burst and collapse load re-calculation of the production casing.

As seen from Fig. 10, the burst and collapse failure occurred at the production casing in this well.

Eq. (4) was used to calculate the buoyancy factor. Lost circulation needed to be considered in the tension load case identification since it caused a fluctuation in the buoyancy factor. Table 5 shows the fluctuation of the buoyancy factor due to lost circulation.

The rate of lost circulation as shown in Table 5 considered in the re-calculation were 0, 50%, and 100% (total lost circulation). The tension load was calculated based on the tension rating of the production casing, the buoyancy factor in Table 5, and the design factor. The design factor for tension load re-calculation was 2.2 (Hole, 2008; Marbun, 2013). The yield correction factor from the New Zealand Standard NZS 2403:2015 was then applied to the tension rating of the casing (Standards New Zealand, 2015). Fig. 11 shows the tension load re-calculation of the production casing.

As seen from Fig. 11, no tension failure was identified.

A similar re-calculation procedure for burst, collapse, and tension loads was applied for the other casing installed in this well. Table 6 shows a summary of casing design load case identification for all the installed casing.

Seen from Table 6, burst and collapse failure occurred at the actual casing installed in this well.

4.3. Thermal expansion evaluation of trapped fluid

The original design of this well did not consider the thermal expansion evaluation of the trapped fluid. In this study, the actual production casing installed in this well was then evaluated according to these criteria. Table 7 shows the ratio of the collapse rating of the actual production casing to the burst rating of the actual surface casing.

According to the design factor requirement for thermal expansion due to trapped fluid, the ratio of production casing collapse rating to surface casing burst rating should not be less than 1.2 (Hole, 2008; Southon, 2005). Thus, the actual production casing installed is not appropriate according to these criteria.

4.4. Material selection

The material of the production casing and production liner in this well was evaluated according to corrosion equations developed by Ekasari and Marbun (2015). Eq. (5) was used to calculate the Cr_{eq} value. The Cr_{eq} diagram was then established based on the temperature, the average pH data of the fluid (pH 4), and the corrosion rate target (0.1 mm/year). Fig. 12 shows the Cr_{eq} diagram for production casing and production liner.

The figure of Cr_{eq} then was matched with range of Cr_{eq} shown in Table 1. It was then determined that the suitable material for production casing and production liner was M65 or higher.

Table 8 shows the corrosion assessment summary of actual production casing and production liner of this well.

As can be seen from Table 8, the material of production casing of this well was not suitable based on the corrosion assessment.

5. Conclusion

The re-calculation of casing setting depth and design of well HCE29 shows that the burst and collapse failure occurred in the actual surface casing, production casing, and production liner of the well. The actual production casing was not appropriate based on the thermal expansion evaluation of trapped fluid analysis, and the material of the actual production casing of this well was also not suitable based on the corrosion assessment and material selection analysis.

The casing setting depth and design should be based on the actual load encountered during various phases such as drilling and completion, production, maintenance (well intervention, and workover), conversion into an injection well or vice-versa, and P&A. This also includes other variables such as geothermal environment (high temperature and presence of corrosive fluid), the well configuration, problems and hazards encountered in

Table 7
Thermal expansion of trapped fluid calculation of the well.

Yield correction factor at max. temperature	Corrected collapse rating for production casing (MPa) (A)	Corrected burst rating for Surface casing (MPa) (B)	Ratio (A)/(B)	Criteria fulfilled?
0.728	9.8	12.1	0.81	✖

Table 8
Production casing and production liner corrosion assessment.

Casing	Temperature (°C)	Cr_{eq}	Minimum casing material	Actual casing material	Criteria fulfilled?
Production casing	337	−4.884	M65	K55	✖
Production liner	338	−4.884	M65	L80	✓

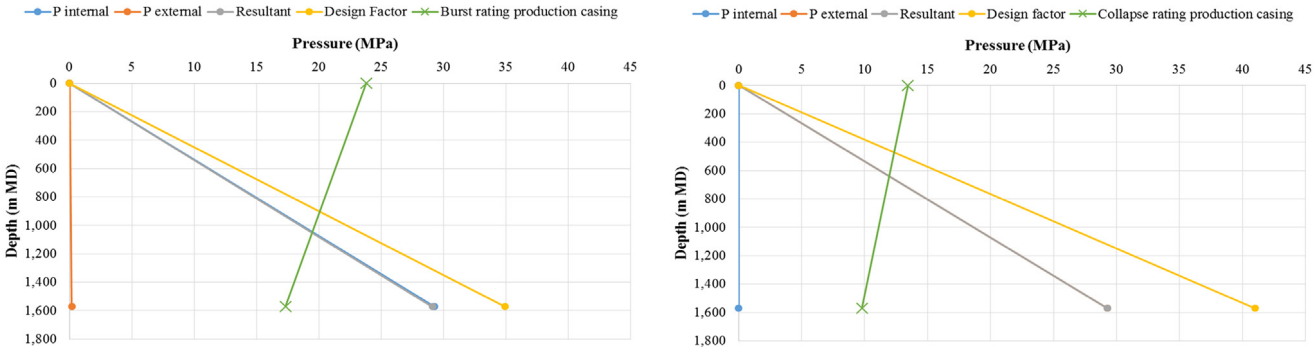

Fig. 10. The burst (left) and collapse (right) load re-calculation of the production casing in the well.

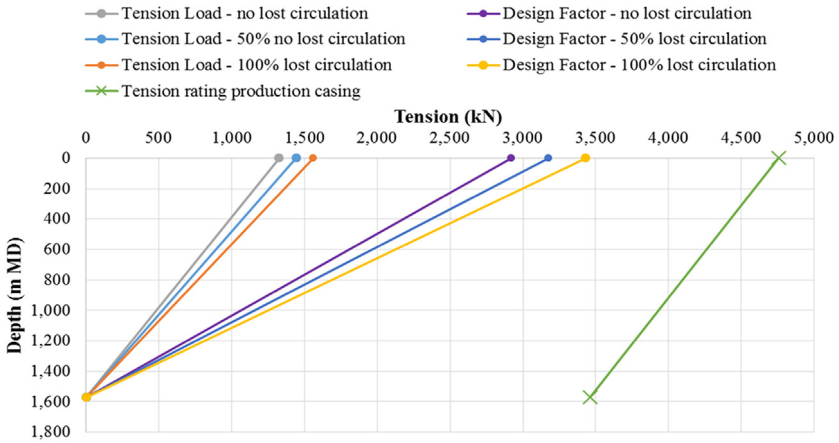

Fig. 11. The tension load re-calculation of production casing in the well.

each section depth (such as high dogleg severity (DLS) and lost circulation) that significantly affect the load experienced by the casing and the casing material degradation. Furthermore, the American Petroleum Institute (API) casing is common to be utilized in geothermal well in Indonesia. Correction or adjustment of material strength should be made when the API casing is used in the geothermal well (e.g., high-temperature effect). This study considers not only the high reservoir temperature (220 °C), but also the maximum load for casing setting depth and design from the phases analyzed in well HCE29, including various pressure and temperature survey data, well problems (high DLS and lost circulation), lithologic and geologic, production, and casing material. These parameters are not considered in the Philippines' method, since it only considers high reservoir temperature, which is 220 °C, for casing setting depth.

The evaluation methodology of casing design and setting depth in this study was established comprehensively in the working flow chart, including data analysis, casing setting depth,

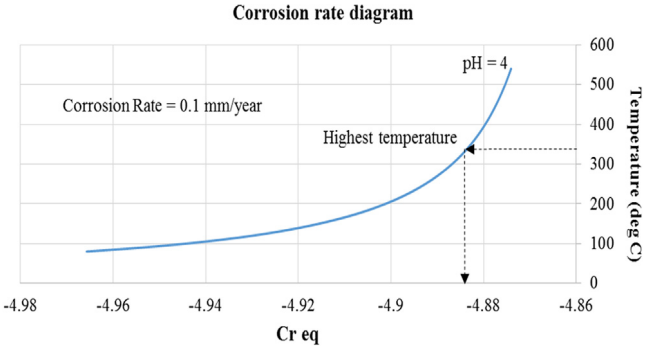

Fig. 12. Cr_{eq} rate diagram of production casing the well.

casing design load case identification, casing grade selection, thermal expansion due to trapped fluid evaluation, material selection, lesson learned, and the advancement of SOP. In addition, the results show that the methodology is also useful to investigate the casing failure in the actual geothermal well. The lesson learned from this study and the advancement of SOP are useful and fruitful for future geothermal well casing design in Dieng Field.

6. Recommendations

From the findings and discussion of the study, the following recommendations are proposed:

1. The casing setting depth and design in geothermal Dieng Field have to be considered not only in the drilling and the completion phase, but also in the production, maintenance (well intervention and workover), the conversion into an injection well or vice-versa, and the plug and abandon (P&A) phase.
2. The casing grade and material selection must be conducted properly and precisely according to the formation condition and fluid in geothermal Dieng Field.
3. Based on the casing setting depth analysis using the Philippines' method improved in this study, the following particular suggestion can be proposed: one additional section of intermediate production casing/liner can be considered in the future based on engineering and economic considerations.

List of abbreviations and nomenclature

APB:	Annular pressure build-up	HSO_4^-:	Hydrogen sulfate
API:	American petroleum institute	H_2S:	Hydrogen sulfide
ASTM:	American Standard Testing and Material	Lnr:	Liner
BPD:	Boiling point depth	NH_3:	Ammonia
		NH_4Cl:	Ammonium chloride
BTC:	Buttress thread connection	NZS:	New Zealand Standard
Csg:	Casing	MD:	Measured depth (m)
CO_2:	Carbon dioxide	P&A:	Plug and abandon
CO_3^{2-}:	Carbonate	TFT	Tracer flow test
CRA:	Corrosion resistant alloy	TOL:	Top of liner
DLS:	Dogleg severity	TVD:	True vertical depth (m)
HCl:	Hydrogen chloride	SiO_2:	Silicon dioxide
HCO_3^-:	Bicarbonate	SOP:	Standard operating procedure
HSE:	Health, safety, and environment	WHP:	Wellhead pressure (MPa, bar)

Declaration of competing interest

The authors declare that they have no known competing financial interests or personal relationships that could have appeared to influence the work reported in this paper.

CRediT authorship contribution statement

B.T.H. Marbun: Conceptualization, Data curation, Formal analysis, Funding acquisition, Investigation, Methodology, Project administration, Resources, Software, Supervision, Validation, Visualization, Writing - original draft, Writing - review & editing. **R.H. Ridwan:** Project administration, Resources. **H.S. Nugraha:** Project administration, Resources. **S.Z. Sinaga:** Software, Supervision, Validation, Visualization, Writing - original draft, Writing - review & editing. **B.A. Purbantanu:** Software, Supervision, Validation, Visualization, Writing - original draft, Writing - review & editing.

Acknowledgment

The authors would like to express their sincere gratitude to PT Geo Dipa Energi for giving the permission to publish this project.

References

American Petroleum Institute (API), American Petroleum Institute (API), 1998. API RP 7G: Recommended Practice for Drill Stem Design and Operating Limits, sixteenth ed. American Petroleum Institute (API), Washington, D.C..
American Petroleum Institute (API), 2005. API Spec 10 a: Specification for Cements and Materials for Well Cementing, tweenty-third ed. American Petroleum Institute (API), Washington, D.C..
American Petroleum Institute (API), 2011. API Spec 5CT: Specification for Casing and Tubing, ninth ed. American Petroleum Institute, Washington, D.C..
American Standard Testing and Material (ASTM), 2017. ASTM A193/A193M Standard Specification for Alloy-Steel and Stainless Steel Bolting for High Temperature Or High Pressure Service and Other Special Purpose Applications. ASTM International, West Conshohocken, PA.
Bourgoyne Jr., A., Millheim, K., Chenevert, M., Young Jr., F., 1986. Applied Drilling Engineering, Vol. 2. Society of Petroleum Engineers, Richardson, Texas,
Byrom, T., 2007. Casing and Liners for Drilling and Completion. Gulf Publishing Company, Houston, Texas.
Cabrini, M., Lorenzi, S., Pastore, T., Favilla, M., Perini, R., Tarquini, B., 2017. Materials selection for dew-point corrosion in geothermal fluids containing acid chloride. Geothermics 69, 139–144.
Dench, N., 1970. Casing string design for geothermal wells. Geothermics 2, 1485–1496.
Dinçer, I., Acar, A., Çobanoğlu, I., Uras, Y., 2004. Correlation between Schmidt hardness, uniaxial compressive strength and Young's modulus for andesites, basalts and tuffs. Bull. Eng. Geol. Environ. 63 (2), 141–148.
Dong, G., Chen, P., 2017. A review of the evaluation methods and control technologies for trapped annular pressure in deepwater oil and gas wells. J. Natural Gas Sci. Eng. 37, 85–105.
Ekasari, N., Marbun, B., 2015. Integrated analysis of optimizing casing materials selection of geothermal well by using a model for calculating corrosion rates. In: World Geothermal Congress, Melbourne, Australia.
Ellis, P.I., Conover, M., 1981. Materials Selection Guidelines for Geothermal Energy Utilization Systems. Report for the US DOE Washington,.
Hole, H., 2008. Geothermal well design – Casing and wellhead, In: Petroleum Engineering Summer School, Dubrovnik, Croatia.
Hossein-Pourazad, H., 2005. High-temperature geothermal well design. In: The United Nations University Geothermal Training Programme, Reykjavik, Iceland.
Kaldal, G., Jonsson, M., Palsson, H., Karlsdottir, S., 2015. Structural modeling of the casings in high temperature geothermal wells. Geothermics 55, 126–137.
Karlsdottir, S., Ragnarsdottir, K., Thorbjornsson, I., Einarsson, A., 2015. Corrosion testing in superheated geothermal steam in iceland. Geothermics 53, 281–290.
Karlsson, T., 1978. Casing design for high temperature geothermal wells. Geotherm. Resour. Counc. Trans. 2, 355–358.
Kermani, B., Gonzales, J., Turconi, G., Perez, T., Morales, C., 2005. Materials optimisation in hydrocarbon production. In: Corrosion 3-7 2005, Houston, Texas.
Kurata, Y., Sanada, N., Nanjo, H., Ikeuchi, J., 1995. Casing pipe materials for deep geothermal wells. Geotherm. Resour. Counc. Trans. 19, 105–109.
Mahon, T., Harvey, C., Crosby, D., 2000. The chemistry of geothermal fluids in indonesia and their relationship to water and vapour dominated systems. In: World Geothermal Congress, Kyushu - Tohoku, Japan.
Marbun, B., 2013. Final Report: Wellbore Problem Identification and Workover Feasibility Study of Dieng Geothermal Field, Indonesia, PT Geo Dipa Energi. Bandung Institute of Technology, Bandung, Indonesia.
Marbun, B., Ridwan, R., Sinaga, S., Pande, B., Purbantanu, B., 2019. Casing failure identification of long-abandoned geothermal wells in field dieng, Indonesia. Geotherm. Energy 7 (31).
Nicholson, R., 1984. Casing design for temperature regimes in geothermal wells. Geotherm. Resour. Counc. Bull. 23–26, Vols. 1984-May.
Nogara, J., Zarrouk, S., 2018a. Corrosion in geothermal environment: Part 1: Fluids and their impact. Renew. Sustain. Energy Rev. 82, 1333–1346.
Nogara, J., Zarrouk, S., 2018b. Corrosion in geothermal environment part 2: Metals and alloys. Renew. Sustain. Energy Rev. 82, 1347–1369.

Perras, M., Diederichs, M., 2014. A review of the tensile strength of rock: Concepts and testing. Geotech. Geol. Eng. 32 (2), 525–546.
PT Geo Dipa Energi, 2019. Internal Report. Geo Dipa Energi, Jakarta.
Rahman, S., Chilingarian, G., 1995. Casing design - Theory and practice. In: Develepments in Petroleum Science, Vol. 42, first ed. Elsevier Science B.V., Amsterdam.
Sarmiento, Z., 2007. A snapshot of the drilling and completion practices in high temperature geothermal wells in the Philippines. In: Workshop 4 of the Engine Drilling cost effectiveness and feasibility of high-temperature drilling, Reykjavik, Iceland.
Smith, L., DeWaard, C., 2005. Corrosion prediction and materials selection for oil and gas producing environments, In: Corrosion 3-7 April 2005, Houston, Texas.
Southon, J., 2005. Geothermal well design, construction and failures. In: World Geothermal Congress 2005, Antalya, Turkey.
Standards New Zealand, 1991. NZS 2403:1991-New Zealand Standard, Code of Practice for Deep Geothermal Wells. Standard Association of New Zealand, Wellington.
Standards New Zealand, 2015. NZS 2403:2015-New Zealand Standard, Code of Practice for Deep Geotehrmal Wells. Standards New Zealand, Wellington.
Zhang, B., Guan, Z., Lu, N., Hasan, A., Wang, Q., Xu, B., 2019. Trapped annular pressure caused by thermal expansion in oil and gas wells: A review of prediction approaches, risk assessment and mitigation strategies. J. Pet. Sci. Eng. 172, 70–82.